

## A POSTERIORI ERROR ESTIMATES FOR LOCAL $C^0$ DISCONTINUOUS GALERKIN METHODS FOR KIRCHHOFF PLATE BENDING PROBLEMS\*

Yifeng Xu

*Department of Mathematics, Shanghai Normal University, Shanghai 200234, China*  
*Division of Computational Science, E-Institute of Shanghai Universities, Shanghai Normal*  
*University, Shanghai 200234, China*  
*Scientific Computing Key Laboratory of Shanghai Universities, Shanghai Normal University,*  
*Shanghai 200234, China*  
*Email: yfxu@shnu.edu.cn*

Jianguo Huang

*Department of Mathematics, MOE-LSC, Shanghai Jiao Tong University, Shanghai 200240, China*  
*Division of Computational Science, E-Institute of Shanghai Universities, Shanghai Normal*  
*University, Shanghai 200234, China*  
*Email: jghuang@sjtu.edu.cn*

Xuehai Huang

*College of Mathematics and Information Science, Wenzhou University, Wenzhou 325035, China*  
*Email: xuehaihuang@wzu.edu.cn*

### Abstract

We derive some residual-type a posteriori error estimates for the local  $C^0$  discontinuous Galerkin (LCDG) approximations ([31]) of the Kirchhoff bending plate clamped on the boundary. The estimator is both reliable and efficient with respect to the moment-field approximation error in an energy norm. Some numerical experiments are reported to demonstrate theoretical results.

*Mathematics subject classification:* 65N15, 65N30.

*Key words:* Kirchhoff bending plate, Discontinuous Galerkin method, A posteriori error analysis.

### 1. Introduction

Over the past two decades, discontinuous Galerkin (DG) methods have been attracting considerable attention as a flexible and efficient computational scheme for many kinds of problems arising in physics and engineering, including linear and nonlinear hyperbolic problems, Navier-Stokes equations, convection-dominated diffusion problems and Maxwell equations; see e.g., [21] and the references therein. A very extensive and thorough study has been done in solving second-order equations/systems by DG methods ([2, 11, 16, 18, 20], to name but a few).

For fourth order problems, e.g., the biharmonic equation and the Kirchhoff plate bending problem, the research dates back to the 1970s [3, 4] and focuses on the interior penalty (IP) methods [10, 23, 24, 27, 34–36, 39]. Based on the ideas in [16, 20] for second order problems, there have developed in [31] a general framework, covering methods in [10, 41], of constructing stable  $C^0$  discontinuous Galerkin (CDG) methods for solving the Kirchhoff plate bending problem.

---

\* Received July 10, 2013 / Revised version received April 4, 2014 / Accepted May 26, 2014 /  
Published online September 3, 2014 /

With some parameter, precisely  $C_{22}$ , taken to be zero in determining numerical traces, a so-called local  $C^0$  discontinuous Galerkin (LCDG) method follows, which may be viewed as an extension of the local discontinuous Galerkin (LDG) method in [16, 20] to fourth order elliptic problems. In addition, optimal-order a priori error estimates for the displacement field in certain discrete energy norm and  $H^1$ -norm are established in [31]. It is also worth mentioning that in a recent work [19] a new DG method, called LDG-Hybridizable Galerkin method, is applied to the biharmonic problem and the a priori error estimates are derived. Although this method is formulated as a first-order system approximating four variables simultaneously, the globally coupled degrees of freedom are only two of them on the faces of the elements so that the implementation is very efficient.

As is known to all, DG methods are well-suited for use in adaptive algorithms, which are usually based on a posteriori error estimates measuring actual discretization errors without recourse to the exact solution and providing information on where a local refinement is required. There have been great and rapid advances in the theory of a posteriori error analysis for second order elliptic problems. In [5], Becker, Hansbo and Larson derived a residual-based reliable error estimate in certain mesh-dependent energy norm for IP methods with the help of the Helmholtz decomposition. Later with a similar technique applied, a reliable a posteriori error estimate for the LDG method was presented in [13]. Further results concerning the issue are available in [1, 14, 15, 29, 32, 37].

Very recently, Hansbo and Larson [28] developed a reliable a posteriori bound of the energy-norm displacement error for a  $C^0$  interior penalty method for the Kirchhoff bending plate by means of a Helmholtz decomposition of second order tensor fields due to Beirão da Veiga et al [6]. We remark in passing that the decomposition had been originally proposed to construct the residual-based a posteriori error estimate of the nonconforming Morley plate bending element [33], which was then improved in [30] and was extended to the case of general boundary conditions [7]. A different approach [25] was taken in treating the case of a fully discontinuous interior penalty method [24], where the derivation of the reliability bound heavily depends on a suitable recovery operator mapping discontinuous finite element spaces into  $H_0^2$ -conforming spaces composed of high-order versions of the classical Hsieh-Clough-Tochner macro-element defined in [22]. The idea was also applied to establish an a posteriori bound for a quadratic  $C^0$  interior penalty method for the biharmonic problem [8].

The aim of this paper is to construct reliable and efficient residual-based a posteriori error estimates of the moment-field error in an energy norm for the LCDG methods in [31]. Similar to the approach in [28], we make use of the Helmholtz decomposition in [6] to deduce the reliability (the upper bound). Particularly, two improved bounds are available when the orders of discrete spaces approximating the moment field and the displacement field satisfy some relation. As regards the efficiency (the lower bound), we follow the traditional lines [40] to bound all error indicators except the jump term with respect to the normal derivative of the approximating displacement field from above by the moment-field error in the energy norm plus the data oscillation.

The rest of the paper is organized as follows. In Section 2, we review the local  $C^0$  discontinuous Galerkin methods for the Kirchhoff plate bending problem. An a posteriori error analysis is performed in Section 3. Finally, in Section 4 we report some numerical examples to illustrate the effectiveness of the error estimator.

We conclude the introduction with some basic notations used in the sequel. Given a bounded domain  $\omega \subset \mathbb{R}^2$ , we will use the usual  $L^2$ -based Sobolev space  $H^s(\omega)$  ( $s \geq 0$ ) unless specified.

The corresponding norm and semi-norm are denoted by  $\|\cdot\|_{s,\omega}$  and  $|\cdot|_{s,\omega}$ , respectively. If  $\omega$  is  $\Omega$ , we abbreviate them by  $\|\cdot\|_s$  and  $|\cdot|_s$ .  $H_0^s(\omega)$  serves as the closure of  $C_0^\infty(\omega)$  with respect to the norm  $\|\cdot\|_{s,\omega}$ .  $L_0^2(\Omega)$  (resp.  $\tilde{H}^1(\Omega)$ ) consists of the functions in  $L^2(\Omega)$  (resp.  $H^1(\Omega)$ ) with zero average over the domain  $\Omega$ . The symbol “:” indicates the double dot product operation of two second order tensor fields. Given an integer  $m \geq 0$ ,  $P_m(\omega)$  denotes the set of all polynomial of degree at most  $m$  on  $\omega$ . For any Banach space  $B$ ,  $(B)_{2 \times 2}^s$  consists of all symmetric second order tensor fields with each component in  $B$ .  $C$  denotes a generic constant independent of the functions under consideration and may be different at each occurrence. Finally, for any scalar field  $v$ , vector field  $\phi$  and second order tensor field  $\tau$ , various differential operators in need are defined below:

$$\begin{aligned} \nabla v &= \begin{pmatrix} \partial_1 v \\ \partial_2 v \end{pmatrix}, \quad \mathbf{curl} v = \begin{pmatrix} -\partial_2 v \\ \partial_1 v \end{pmatrix}; \\ \nabla \phi &= \begin{pmatrix} \partial_1 \phi_1 & \partial_2 \phi_1 \\ \partial_1 \phi_2 & \partial_2 \phi_2 \end{pmatrix}, \quad \mathbf{Curl} \phi = \begin{pmatrix} -\partial_2 \phi_1 & \partial_1 \phi_1 \\ -\partial_2 \phi_2 & \partial_1 \phi_2 \end{pmatrix}, \quad \mathbf{div} \phi = \partial_1 \phi_1 + \partial_2 \phi_2; \\ \mathbf{div} \tau &= \begin{pmatrix} \partial_1 \tau_{11} + \partial_2 \tau_{12} \\ \partial_1 \tau_{21} + \partial_2 \tau_{22} \end{pmatrix}, \quad \mathbf{rot} \tau = \begin{pmatrix} \partial_1 \tau_{12} - \partial_2 \tau_{11} \\ \partial_1 \tau_{22} - \partial_2 \tau_{21} \end{pmatrix}. \end{aligned}$$

## 2. The Local $C^0$ Discontinuous Galerkin Method

In this section, an LCDG method for the Kirchhoff plate bending problem is reviewed in brief. We refer to [31] for more details on deriving the numerical scheme.

Let  $\Omega$  denote a polygon domain in  $\mathbb{R}^2$  occupied by the midsection of a plate. The clamped Kirchhoff plate bending model subject to a vertical load density  $f \in L^2(\Omega)$  reads: find the displacement field  $u$  such that

$$\begin{cases} -\mathbf{div} \mathbf{div} \mathcal{M}(u) = f & \text{in } \Omega, \\ u = \partial_n u = 0 & \text{on } \partial\Omega, \end{cases} \tag{2.1}$$

where the symmetric second order tensor field  $\mathcal{M}(u)$  standing for the moment field satisfies the Hooke’s law:

$$\begin{aligned} \mathcal{M}(u) &:= \frac{Ed^3}{12(1-\nu^2)} ((1-\nu)\mathcal{K}(u) + \nu \text{tr}(\mathcal{K}(u))\mathcal{I}), \\ \mathcal{K}(u) &:= -(\partial_{ij} u)_{ij}, \quad i, j = 1, 2, \end{aligned} \tag{2.2}$$

with the constants  $d$ ,  $E$  and  $\nu \in (0, 0.5)$  being the thickness, the Young’s modulus, and the Poisson’s ratio of the plate respectively,  $\mathbf{n}$  is the unit normal outward to  $\partial\Omega$  and  $\mathcal{I}$  is the identity matrix. The corresponding variational problem takes the form: Find  $u \in H_0^2(\Omega)$  such that

$$\int_{\Omega} \mathcal{M}(u) : \mathcal{K}(v) dx = \int_{\Omega} f v dx \quad \forall v \in H_0^2(\Omega). \tag{2.3}$$

Introducing an auxiliary  $2 \times 2$  tensor field, by  $\sigma := \mathcal{M}(u)$ , we can reformulate (2.1) as the following second order system:

$$\begin{cases} \mathcal{K}(u) = \mathcal{C}(\sigma), \\ -\mathbf{div} \mathbf{div} \sigma = f & \text{in } \Omega, \\ u = \partial_n u = 0 & \text{on } \partial\Omega, \end{cases} \tag{2.4}$$

where

$$\mathcal{C}(\boldsymbol{\sigma}) = \frac{12(1-\nu^2)}{Ed^3} \left( \frac{1}{1-\nu} \boldsymbol{\sigma} - \frac{\nu}{1-\nu^2} \text{tr}(\boldsymbol{\sigma}) \mathcal{I} \right). \tag{2.5}$$

Next we let  $\mathcal{T}_h$  be a shape regular triangulation of  $\Omega$  into disjoint triangles  $K$  with the diameter  $h_K$ .  $\mathcal{F}_h$  (resp.  $\mathcal{F}_h(\Omega)$ ) denotes the set of all edges in  $\mathcal{T}_h$  (resp. all interior edges) and for each  $F \in \mathcal{F}_h$ ,  $h_F$  is its length. We shall use two finite element spaces associated with  $\mathcal{T}_h$  to approximate the moment field and the displacement field respectively: for integers  $k \geq 1$  and  $l \geq 0$

$$\begin{aligned} \boldsymbol{\Sigma}_h^l &:= \left\{ \boldsymbol{\tau} \in (L^2(\Omega))_{2 \times 2}^s : \tau_{ij}|_K \in P_l(K), \forall K \in \mathcal{T}_h, i, j = 1, 2 \right\}, \\ V_h^k &:= \left\{ v \in H_0^1(\Omega) : v|_K \in P_k(K), \forall K \in \mathcal{T}_h \right\}. \end{aligned}$$

Moreover, to guarantee uniqueness of the solution to the LCDG method presented later, it is assumed that

$$\mathcal{K}_h(V_h^k) \subset \boldsymbol{\Sigma}_h^l, \quad \mathcal{C}(\boldsymbol{\Sigma}_h^l) \subset \boldsymbol{\Sigma}_h^l, \tag{2.6}$$

where  $\mathcal{K}_h(V_h^k)$  is an elementwise version of  $\mathcal{K}(V_h^k)$  on each  $K \in \mathcal{T}_h$  and the same holds true of  $\mathcal{M}_h$  in the sequel.

Before proceeding to the LCDG method, more basic notations are needed. For two vectors  $\mathbf{a}$  and  $\mathbf{b}$ ,  $\mathbf{a} \otimes \mathbf{b}$  represents a second order tensor with  $a_i b_j$  being its  $(i, j)$ -th element. For two adjacent triangles  $K^+$  and  $K^-$  sharing an interior edge  $F$ ,  $\mathbf{n}^+$  and  $\mathbf{n}^-$  are related unit outward normals to  $F$ . For a scalar field  $v$ ,  $v^+$  and  $v^-$  are written for  $v|_{K^+}$  and  $v|_{K^-}$  respectively. The same is also true of a second order tensor field  $\boldsymbol{\tau}$ . Then we define averages and jumps as follows:

$$\begin{aligned} \{v\} &= \frac{1}{2}(v^+ + v^-), & [v] &= v^+ \mathbf{n}^+ + v^- \mathbf{n}^-, \\ \{\nabla v\} &= \frac{1}{2}(\nabla v^+ + \nabla v^-), & [\nabla v] &= \nabla v^+ \cdot \mathbf{n}^+ + \nabla v^- \cdot \mathbf{n}^-, \\ \{\boldsymbol{\tau}\} &= \frac{1}{2}(\boldsymbol{\tau}^+ + \boldsymbol{\tau}^-), & [\boldsymbol{\tau}] &= \boldsymbol{\tau}^+ \mathbf{n}^+ + \boldsymbol{\tau}^- \mathbf{n}^-. \end{aligned}$$

On an edge  $F \subset \partial\Omega$ , the above definitions are given by

$$\begin{aligned} \{v\} &= v, & [v] &= v \mathbf{n}, \\ \{\nabla v\} &= \nabla v, & [\nabla v] &= \nabla v \cdot \mathbf{n}, \\ \{\boldsymbol{\tau}\} &= \boldsymbol{\tau}, & [\boldsymbol{\tau}] &= \boldsymbol{\tau} \mathbf{n}, \end{aligned}$$

where  $\mathbf{n}$  is the unit outward normal on the boundary. Furthermore, the jump  $[[\cdot]]$  of a gradient  $\nabla v$  is defined by

$$\begin{aligned} [[\nabla v]] &= \frac{1}{2}(\nabla v^+ \otimes \mathbf{n}^+ + \mathbf{n}^+ \otimes \nabla v^+ + \nabla v^- \otimes \mathbf{n}^- + \mathbf{n}^- \otimes \nabla v^-), \quad \text{if } F \in \mathcal{F}_h(\Omega), \\ [[\nabla v]] &= \frac{1}{2}(\nabla v \otimes \mathbf{n} + \mathbf{n} \otimes \nabla v), \quad \text{if } F \in \mathcal{F}_h \cap \partial\Omega. \end{aligned}$$

The main idea of the LCDG method is to construct discrete local conservation laws on each  $K \in \mathcal{T}_h$  by replacing the traces of  $\boldsymbol{\sigma}$  and  $\nabla u$  in the continuous counterpart determined by (2.4) on the boundary of each  $K \in \mathcal{T}_h$  with suitable numerical traces  $\widehat{\boldsymbol{\sigma}}_h$  and  $\widehat{\nabla u}_h$ . As in [31], we

consider the following formulation: Find  $(\boldsymbol{\sigma}_h, u_h) \in \boldsymbol{\Sigma}_h^l \times V_h^k$  such that on each  $K \in \mathcal{T}_h$

$$\begin{aligned} \int_K \mathcal{C}(\boldsymbol{\sigma}_h) : \boldsymbol{\tau} dx &= \int_K \mathbf{div} \boldsymbol{\tau} \cdot \nabla u_h dx - \int_{\partial K} \boldsymbol{\tau} \mathbf{n} \cdot \widehat{\nabla} u_h ds \quad \forall \boldsymbol{\tau} \in \boldsymbol{\Sigma}_h^l, \\ \int_K \boldsymbol{\sigma}_h : \mathcal{K}(v) dx + \int_{\partial K} \widehat{\boldsymbol{\sigma}}_h \mathbf{n} \cdot \nabla v ds &= \int_K f v dx \quad \forall v \in V_h^k \end{aligned} \tag{2.7}$$

with

$$\begin{aligned} \widehat{\boldsymbol{\sigma}}_h &= \{\boldsymbol{\sigma}_h\} + \frac{\alpha_{F,h}}{h_F} [[\nabla u_h]], \quad \widehat{\nabla} u_h = \{\nabla u_h\}, \quad \text{if } F \in \mathcal{F}_h(\Omega); \\ \widehat{\boldsymbol{\sigma}}_h &= \boldsymbol{\sigma}_h + \frac{\alpha_{F,h}}{h_F} [[\nabla u_h]], \quad \widehat{\nabla} u_h = 0, \quad \text{if } F \in \mathcal{F}_h \cap \partial\Omega. \end{aligned} \tag{2.8}$$

Here the set  $\{\alpha_{F,h}\}_{F \in \mathcal{F}_h}$  has a uniform positive bound from above and below. After some direct manipulations, the LCDG method based on (2.7) and the numerical traces (2.8) to approximate (2.1), or equivalently (2.4), can be formulated in a mixed formulation as follows: Find  $(\boldsymbol{\sigma}_h, u_h) \in \boldsymbol{\Sigma}_h^l \times V_h^k$  such that for any  $(\boldsymbol{\tau}, v) \in \boldsymbol{\Sigma}_h^l \times V_h^k$

$$\begin{cases} \int_{\Omega} \mathcal{C}(\boldsymbol{\sigma}_h) : \boldsymbol{\tau} dx - \sum_{K \in \mathcal{T}_h} \int_K \boldsymbol{\tau} : \mathcal{K}(u_h) dx - \sum_{F \in \mathcal{F}_h} \int_F \{\boldsymbol{\tau}\} : [[\nabla u_h]] ds = 0, \\ \sum_{K \in \mathcal{T}_h} \int_K \boldsymbol{\sigma}_h : \mathcal{K}(v) dx + \sum_{F \in \mathcal{F}_h} \int_F \{\boldsymbol{\sigma}_h\} : [[\nabla v]] ds + \sum_{F \in \mathcal{F}_h} \frac{\alpha_{F,h}}{h_F} \int_F [[\nabla u_h]] : [[\nabla v]] ds = \int_{\Omega} f v dx. \end{cases} \tag{2.9}$$

The well-posedness of (2.9) as well as the a priori error estimates is shown in [31].

### 3. An a Posteriori Error Analysis for the Moment Field

This section is devoted to deriving reliable and efficient a posteriori error estimates of the moment field. We begin with some preliminaries, particularly the Helmholtz decomposition and definitions of error indicators. Then an upper bound and a lower bound of the moment-field error in terms of the error indicators are presented.

To any given edge  $F \in \mathcal{F}_h(\Omega)$ , we assign a fixed normal unit vector  $\mathbf{n}_F := (n_1, n_2)^T$  and a tangential unit vector  $\mathbf{t}_F := (-n_2, n_1)^T$ .  $\omega_F$  is set to be the union of two elements sharing  $F$ . The same convention is also applicable to  $\partial K$  for all  $K \in \mathcal{T}_h$ . For some  $\mathcal{M}_h \subseteq \mathcal{F}_h$ , we define

$$\eta_h^2(\boldsymbol{\sigma}_h, f, \mathcal{M}_h) := \eta_{h,1}^2(\boldsymbol{\sigma}_h, f, \mathcal{M}_h) + \eta_{h,2}^2(\boldsymbol{\sigma}_h, \mathcal{M}_h)$$

with

$$\begin{aligned} \eta_{h,1}^2(\boldsymbol{\sigma}_h, f, \mathcal{M}_h) &:= \sum_{F \in \mathcal{M}_h \cap \mathcal{F}_h(\Omega)} \left( \sum_{K \in \omega_F} h_K^4 \|f + \mathbf{div} \mathbf{div} \boldsymbol{\sigma}_h\|_{0,K}^2 \right. \\ &\quad \left. + h_F^3 \|[\mathbf{div} \boldsymbol{\sigma}_h \cdot \mathbf{n}_F + \partial_t(\boldsymbol{\sigma}_h)_{nt}]\|_{0,F}^2 + h_F \|[(\boldsymbol{\sigma}_h)_{nn}]\|_{0,F}^2 \right), \end{aligned} \tag{3.1}$$

$$\eta_{h,2}^2(\boldsymbol{\sigma}_h, \mathcal{M}_h) := \sum_{F \in \mathcal{M}_h} \left( \sum_{K \in \omega_F} h_K^2 \|\mathbf{rot} \mathcal{C}(\boldsymbol{\sigma}_h)\|_{0,K}^2 + h_F \|[\mathcal{C}(\boldsymbol{\sigma}_h) \mathbf{t}_F]\|_{0,F}^2 \right), \tag{3.2}$$

$$\eta_{h,J}^2(u_h, \mathcal{M}_h) := \sum_{F \in \mathcal{M}_h} \alpha_{F,h}^2 h_F^{-1} \|[[\nabla u_h]]\|_{0,F}^2, \tag{3.3}$$

where  $(\sigma_h)_{nn} := \mathbf{n}_K^T \sigma_h \mathbf{n}_K$ ,  $(\sigma_h)_{nt} := \mathbf{t}_K^T \sigma_h \mathbf{n}_K$ ;  $[\mathbf{div} \sigma_h \cdot \mathbf{n}_F + \partial_t (\sigma_h)_{nt}]$ ,  $[(\sigma_h)_{nn}]$  and  $[\mathcal{C}(\sigma_h) \mathbf{t}_F]$  are all jumps across an interior edge  $F \in \mathcal{F}_h(\Omega)$  while  $[\mathcal{C}(\sigma_h) \mathbf{t}_F]$  is equal to the value of  $\mathcal{C}(\sigma_h) \mathbf{t}_F$  on a boundary edge  $F \in \mathcal{F}_h \cap \partial\Omega$ . The oscillation is given by

$$\text{osc}_h^2(f, \mathcal{M}_h) = \sum_{K \in \mathcal{M}_h} h_K^4 \|f - \bar{f}_K\|_{0,K}^2$$

for some  $\mathcal{M}_h \subseteq \mathcal{T}_h$ , with  $\bar{f}_K$  being the  $L^2$ -projection of  $f$  onto the constant space  $P_0(K)$  if  $l = 0, 1$  and  $P_{l-2}(K)$  if  $l \geq 2$ . For ease of notation, we further write  $\eta_h^2(\sigma_h, f)$ ,  $\eta_{h,J}^2(u_h)$  and  $\text{osc}_h^2(f)$  for  $\eta_h^2(\sigma_h, f, \mathcal{F}_h)$ ,  $\eta_{h,J}^2(u_h, \mathcal{F}_h)$  and  $\text{osc}_h^2(f, \mathcal{T}_h)$ . And an energy norm  $\|\tau\|_{\mathcal{C}}^2 = \int_{\Omega} \mathcal{C}(\tau) : \tau dx$  is needed for  $\tau \in (L^2(\Omega))_{2 \times 2}^s$ .

To show the reliability, we shall use the following Helmholtz decomposition introduced in [6].

**Lemma 3.1.** *For any second order tensor field  $\tau \in (L^2(\Omega))_{2 \times 2}^s$ , there exist  $\psi \in H_0^2(\Omega)$ ,  $\rho \in L_0^2(\Omega)$  and  $\phi \in (\tilde{H}^1(\Omega))^2$  such that*

$$\tau = \mathcal{M}(\psi) + \rho + \mathbf{Curl} \phi, \tag{3.4}$$

$$(\mathcal{M}(\psi), \mathcal{K}(v)) = (\tau, \mathcal{K}(v)) \quad \forall v \in H_0^2(\Omega), \tag{3.5}$$

where

$$\rho = \begin{pmatrix} 0 & -\rho \\ \rho & 0 \end{pmatrix}. \tag{3.6}$$

Moreover,

$$\|\psi\|_2 + \|\rho\|_0 + \|\phi\|_1 \leq C \|\tau\|_0 \tag{3.7}$$

with the  $C$  depending on the coefficients in  $\mathcal{M}$ .

**Theorem 3.1.** *Let  $\sigma$  and  $\sigma_h$  be solutions of the continuous problem (2.4) and the discrete problem (2.9) respectively. Then there exists a constant  $C_1$  only depending on the shape-regularity of  $\mathcal{T}_h$  and the coefficients in  $\mathcal{C}$ , such that*

$$\|\sigma - \sigma_h\|_{\mathcal{C}}^2 \leq C_1 (\eta_h^2(\sigma_h, f) + \eta_{h,J}^2(u_h)). \tag{3.8}$$

*Proof.* An application of the Helmholtz decomposition (3.4) in Lemma 3.1 to the error tensor  $\sigma - \sigma_h$  gives

$$\begin{aligned} \|\sigma - \sigma_h\|_{\mathcal{C}}^2 &= \int_{\Omega} \mathcal{C}(\sigma - \sigma_h) : \mathcal{M}(\psi) dx + \int_{\Omega} \mathcal{C}(\sigma - \sigma_h) : (\rho + \mathbf{Curl} \phi) dx \\ &:= \mathbf{I}_1 + \mathbf{I}_2, \end{aligned} \tag{3.9}$$

and due to (3.7), it holds

$$\|\psi\|_2 + \|\phi\|_1 \leq C \|\sigma - \sigma_h\|_0. \tag{3.10}$$

Next we handle  $\mathbf{I}_1$  and  $\mathbf{I}_2$  separately. Noting that  $\mathcal{C}$  is the inverse of  $\mathcal{M}$ , making use of (2.3),  $\psi \in H_0^2(\Omega)$  and the second equation of (2.9) with  $v$  taken to be a usual Lagrange interpolant

$I_h^k \psi$  in  $V_h^k$ , and doing an elementwise integration by parts twice, we get

$$\begin{aligned}
 I_1 &= \int_{\Omega} (\boldsymbol{\sigma} - \boldsymbol{\sigma}_h) : \mathcal{K}(\psi) dx \\
 &= \int_{\Omega} f \psi dx - \sum_{K \in \mathcal{T}_h} \int_K \boldsymbol{\sigma}_h : \mathcal{K}(\psi) dx - \sum_{F \in \mathcal{F}_h} \int_F \{\boldsymbol{\sigma}_h\} : [[\boldsymbol{\nabla} \psi]] ds - \sum_{F \in \mathcal{F}_h} \frac{\alpha_{F,h}}{h_F} \int_F [[\boldsymbol{\nabla} u_h]] : [[\boldsymbol{\nabla} \psi]] ds \\
 &= \int_{\Omega} f(\psi - I_h^k \psi) dx - \sum_{K \in \mathcal{T}_h} \int_K \boldsymbol{\sigma}_h : (\mathcal{K}(\psi - I_h^k \psi)) dx - \sum_{F \in \mathcal{F}_h} \int_F \{\boldsymbol{\sigma}_h\} : [[\boldsymbol{\nabla}(\psi - I_h^k \psi)]] ds \\
 &\quad - \sum_{F \in \mathcal{F}_h} \frac{\alpha_{F,h}}{h_F} \int_F [[\boldsymbol{\nabla} u_h]] : [[\boldsymbol{\nabla}(\psi - I_h^k \psi)]] ds \\
 &= \sum_{K \in \mathcal{T}_h} \int_K (f + \text{div div } \boldsymbol{\sigma}_h)(\psi - I_h^k \psi) dx - \sum_{F \in \mathcal{F}_h(\Omega)} \int_F [\text{div } \boldsymbol{\sigma}_h \cdot \mathbf{n}_F](\psi - I_h^k \psi) ds \\
 &\quad + \sum_{K \in \mathcal{T}_h} \int_{\partial K} \boldsymbol{\sigma}_h \mathbf{n} \cdot \boldsymbol{\nabla}(\psi - I_h^k \psi) ds - \sum_{F \in \mathcal{F}_h} \int_F \{\boldsymbol{\sigma}_h\} : [[\boldsymbol{\nabla}(\psi - I_h^k \psi)]] ds \\
 &\quad - \sum_{F \in \mathcal{F}_h} \frac{\alpha_{F,h}}{h_F} \int_F [[\boldsymbol{\nabla} u_h]] : [[\boldsymbol{\nabla}(\psi - I_h^k \psi)]] ds. \tag{3.11}
 \end{aligned}$$

Now we turn our attention to the term  $\sum_{K \in \mathcal{T}_h} \int_{\partial K} \boldsymbol{\sigma}_h \mathbf{n} \cdot \boldsymbol{\nabla}(\psi - I_h^k \psi) ds$ . As  $\psi$  and  $I_h^k \psi$  agree at all vertices of  $\mathcal{T}_h$  and  $\psi - I_h^k \psi$  is continuous across all  $F \in \mathcal{F}_h(\Omega)$ , a direct manipulation leads to

$$\begin{aligned}
 &\sum_{K \in \mathcal{T}_h} \int_{\partial K} \boldsymbol{\sigma}_h \mathbf{n} \cdot \boldsymbol{\nabla}(\psi - I_h^k \psi) ds \\
 &= \sum_{F \in \mathcal{F}_h(\Omega)} \int_F [\boldsymbol{\sigma}_h] \cdot \{\boldsymbol{\nabla}(\psi - I_h^k \psi)\} ds + \sum_{F \in \mathcal{F}_h} \int_F \{\boldsymbol{\sigma}_h\} : [[\boldsymbol{\nabla}(\psi - I_h^k \psi)]] ds \\
 &= - \sum_{F \in \mathcal{F}_h(\Omega)} \int_F [\partial_t(\boldsymbol{\sigma}_h)_{nt}](\psi - I_h^k \psi) ds + \sum_{F \in \mathcal{F}_h(\Omega)} \int_F [(\boldsymbol{\sigma}_h)_{nn}] \{\partial_n(\psi - I_h^k \psi)\} ds \\
 &\quad + \sum_{F \in \mathcal{F}_h} \int_F \{\boldsymbol{\sigma}_h\} : [[\boldsymbol{\nabla}(\psi - I_h^k \psi)]] ds. \tag{3.12}
 \end{aligned}$$

Substituting (3.12) into (3.11), we proceed

$$\begin{aligned}
 I_1 &= \sum_{K \in \mathcal{T}_h} \int_K (f + \text{div div } \boldsymbol{\sigma}_h)(\psi - I_h^k \psi) dx - \sum_{F \in \mathcal{F}_h(\Omega)} \int_F [\text{div } \boldsymbol{\sigma}_h \cdot \mathbf{n}_F \\
 &\quad + \partial_t(\boldsymbol{\sigma}_h)_{nt}](\psi - I_h^k \psi) ds + \sum_{F \in \mathcal{F}_h(\Omega)} \int_F [(\boldsymbol{\sigma}_h)_{nn}] \{\partial_n(\psi - I_h^k \psi)\} ds \\
 &\quad - \sum_{F \in \mathcal{F}_h} \frac{\alpha_{F,h}}{h_F} \int_F [[\boldsymbol{\nabla} u_h]] : [[\boldsymbol{\nabla}(\psi - I_h^k \psi)]] ds. \tag{3.13}
 \end{aligned}$$

With the help of the Cauchy-Schwarz inequality and the interpolation error estimates for  $I_h^k$  (cf. [9,17]), we obtain

$$I_1 \leq C \left( \eta_{h,1}(\boldsymbol{\sigma}_h, f) + \eta_{h,J}(u_h) \right) \|\psi\|_2. \tag{3.14}$$

Regarding  $I_2$ , we first use the relation  $\mathcal{C}(\boldsymbol{\sigma}) = \mathcal{K}(u)$ , the definition of the tensor field  $\boldsymbol{\rho}$  and an integration by parts to get

$$I_2 = \int_{\Omega} \mathcal{C}(\boldsymbol{\sigma} - \boldsymbol{\sigma}_h) : (\boldsymbol{\rho} + \mathbf{Curl}\boldsymbol{\phi}) dx = - \int_{\Omega} \mathcal{C}(\boldsymbol{\sigma}_h) : (\boldsymbol{\rho} + \mathbf{Curl}\boldsymbol{\phi}) dx. \tag{3.15}$$

Then invoking the vectorial Scott-Zhang interpolation operator  $\mathbf{I}_h^{s,l+1} : (H^1(\Omega))^2 \rightarrow \mathbf{V}_h^{l+1}$  [38], where  $\mathbf{V}_h^{l+1} := \{\mathbf{v} \in (H^1(\Omega))^2 \mid \mathbf{v}|_K \in (P_{l+1}(K))^2 \forall K \in \mathcal{T}_h\}$ , we obtain  $\mathbf{I}_h^{s,l+1}\boldsymbol{\phi} \in \mathbf{V}_h^{l+1}$  and construct a tensor field  $\boldsymbol{\rho}_h$  by

$$\boldsymbol{\rho}_h = \begin{pmatrix} 0 & -\rho_h \\ \rho_h & 0 \end{pmatrix}$$

with  $\rho_h = \frac{1}{2} \operatorname{div}(\mathbf{I}_h^{s,l+1}\boldsymbol{\phi})$ . It is not difficult to check that  $\boldsymbol{\rho}_h + \mathbf{Curl}\mathbf{I}_h^{s,l+1}\boldsymbol{\phi} \in \boldsymbol{\Sigma}_h^l$ . Furthermore, by the definition of  $[[\nabla u_h]]$  and the fact that  $u_h \in H_0^1(\Omega)$ , it holds on each  $F \in \mathcal{F}_h$

$$\begin{aligned} [[\nabla u_h]] &= \left( [[\nabla u_h]] : \mathbf{n}_F \otimes \mathbf{n}_F \right) \mathbf{n}_F \otimes \mathbf{n}_F + \left( [[\nabla u_h]] : \mathbf{t}_F \otimes \mathbf{n}_F \right) \mathbf{n}_F \otimes \mathbf{t}_F \\ &\quad + \left( [[\nabla u_h]] : \mathbf{n}_F \otimes \mathbf{t}_F \right) \mathbf{t}_F \otimes \mathbf{n}_F + \left( [[\nabla u_h]] : \mathbf{t}_F \otimes \mathbf{t}_F \right) \mathbf{t}_F \otimes \mathbf{t}_F \\ &= [\nabla u_h] \mathbf{n}_F \otimes \mathbf{n}_F + [\nabla u_h \cdot \mathbf{t}_F] \mathbf{n}_F \otimes \mathbf{t}_F + [\nabla u_h \cdot \mathbf{t}_F] \mathbf{t}_F \otimes \mathbf{n}_F + 0 \\ &= [\nabla u_h] \mathbf{n}_F \otimes \mathbf{n}_F, \end{aligned}$$

where  $[\nabla u_h \cdot \mathbf{t}_F]$  is the jump across interior edges and takes the value of  $\nabla u_h \cdot \mathbf{t}_F$  on boundary edges. Noting the antisymmetry of  $\boldsymbol{\rho}_h$ , the definition of  $\{\boldsymbol{\rho}_h\}$  and the symmetry of  $[[\nabla u_h]]$ , we have

$$\sum_{K \in \mathcal{T}_h} \int_K \boldsymbol{\rho}_h : \mathcal{K}(u_h) dx + \sum_{F \in \mathcal{F}_h} \int_F \{\boldsymbol{\rho}_h\} : [[\nabla u_h]] ds = 0. \tag{3.16}$$

Since

$$\operatorname{div}(\mathbf{Curl}\mathbf{I}_h^{s,l+1}\boldsymbol{\phi}) = \mathbf{0}, \quad (\mathbf{Curl}\mathbf{I}_h^{s,l+1}\boldsymbol{\phi})\mathbf{n}_K = -(\nabla\mathbf{I}_h^{s,l+1}\boldsymbol{\phi})\mathbf{t}_K \quad \forall K \in \mathcal{T}_h,$$

we also have

$$\begin{aligned} &\sum_{K \in \mathcal{T}_h} \int_K \mathbf{Curl}\mathbf{I}_h^{s,l+1}\boldsymbol{\phi} : \mathcal{K}(u_h) dx \\ &= \sum_{K \in \mathcal{T}_h} \left( \int_K \operatorname{div}(\mathbf{Curl}\mathbf{I}_h^{s,k+1}\boldsymbol{\phi}) \cdot \nabla u_h dx - \int_{\partial K} (\mathbf{Curl}\mathbf{I}_h^{s,k+1}\boldsymbol{\phi})\mathbf{n}_K \cdot \nabla u_h ds \right) \\ &= - \sum_{F \in \mathcal{F}_h} \int_F \mathbf{n}_F^T (\mathbf{Curl}\mathbf{I}_h^{s,k+1}\boldsymbol{\phi}) \mathbf{n}_F [\nabla u_h] ds. \end{aligned} \tag{3.17}$$

On the other hand, using the representation of  $[[\nabla u_h]]$  given above and the continuity of  $\mathbf{I}_h^{s,l+1}\boldsymbol{\phi}$  across all interior edges we find

$$\sum_{F \in \mathcal{F}_h} \int_F \{\mathbf{Curl}\mathbf{I}_h^{s,l+1}\boldsymbol{\phi}\} : [[\nabla u_h]] ds = \sum_{F \in \mathcal{F}_h} \int_F \mathbf{n}_F^T (\mathbf{Curl}\mathbf{I}_h^{s,k+1}\boldsymbol{\phi}) \mathbf{n}_F [\nabla u_h] ds. \tag{3.18}$$

Now from the first equation of (2.9) with  $\boldsymbol{\tau} = \boldsymbol{\rho}_h + \mathbf{Curl}\mathbf{I}_h^{s,l+1}\boldsymbol{\phi}$  and (3.16)-(3.18) we know

$$\int_{\Omega} \mathcal{C}(\boldsymbol{\sigma}_h) : (\boldsymbol{\rho}_h + \mathbf{Curl}\mathbf{I}_h^{s,l+1}\boldsymbol{\phi}) dx = 0. \tag{3.19}$$

Subtracting (3.19) from (3.15) and noting the antisymmetry of the tensor field  $\boldsymbol{\rho}$ , we arrive at

$$\begin{aligned} \text{I}_2 &= - \int_{\Omega} \mathcal{C}(\boldsymbol{\sigma}_h) : (\boldsymbol{\rho} - \boldsymbol{\rho}_h + \mathbf{Curl}(\boldsymbol{\phi} - \mathbf{I}_h^{s,l+1}\boldsymbol{\phi})) dx \\ &= - \int_{\Omega} \mathcal{C}(\boldsymbol{\sigma}_h) : \mathbf{Curl}(\boldsymbol{\phi} - \mathbf{I}_h^{s,l+1}\boldsymbol{\phi}) dx. \end{aligned} \tag{3.20}$$

Using an elementwise integration by parts, the error estimates of the Scott-Zhang interpolation operator [38], and the Cauchy-Schwarz inequality, we are further led to

$$\begin{aligned} |\text{I}_2| &= \left| \sum_{K \in \mathcal{T}_h} \int_K \mathbf{rot} \mathcal{C}(\boldsymbol{\sigma}_h) : (\boldsymbol{\phi} - \mathbf{I}_h^{s,l+1}\boldsymbol{\phi}) dx - \sum_{F \in \mathcal{F}_h} \int_F [\mathcal{C}(\boldsymbol{\sigma}_h) \mathbf{t}_F] : (\boldsymbol{\phi} - \mathbf{I}_h^{s,l+1}\boldsymbol{\phi}) ds \right| \\ &\leq C \eta_{h,2}(\boldsymbol{\sigma}_h) \|\boldsymbol{\phi}\|_1. \end{aligned} \tag{3.21}$$

The proof is completed by collecting (3.9)-(3.10), (3.14) and (3.21). □

When  $l \geq 1$ , we are able to derive an improved estimate on the assumption of  $l = k - 1$ . To be specific, the error indicator  $h_F^3 \|[\mathbf{div} \boldsymbol{\sigma}_h \cdot \mathbf{n}_F + \partial_t(\boldsymbol{\sigma}_h)_{nt}]\|_{0,F}^2$  is not involved in this case. We begin with an interpolation operator  $\tilde{I}_h^k : H^2(\Omega) \cap H_0^1(\Omega) \rightarrow V_h^k$ , which is defined by

$$\begin{cases} \tilde{I}_h^k v(p) = v(p) & \text{for any node } p \text{ in } \bar{\Omega}, \\ \int_F (\tilde{I}_h^k v - v) q ds = 0 & \forall q \in P_{k-2}(F) \text{ and } \forall F \in \mathcal{F}_h \text{ (} k \geq 2\text{)}, \\ \int_K (\tilde{I}_h^k v - v) q dx = 0 & \forall q \in P_{k-3}(K) \text{ and } \forall K \in \mathcal{T}_h \text{ (} k \geq 3\text{)}. \end{cases} \tag{3.22}$$

For this operator, we have the following error estimates, the proofs of which are standard (cf. [9,17]).

**Lemma 3.2.** *Suppose  $v \in H^2(\Omega) \cap H_0^1(\Omega)$ . Then for  $k \geq 0$ ,*

$$\|v - \tilde{I}_h^k v\|_{0,K} \leq Ch_K^2 \|v\|_{2,K} \quad \forall K \in \mathcal{T}_h, \tag{3.23}$$

$$\|\partial_n(v - \tilde{I}_h^k v)\|_{0,F} \leq Ch_F^{1/2} \|v\|_{2,\omega_F} \quad \forall F \in \mathcal{F}_h. \tag{3.24}$$

Now in the proof of Theorem 3.1 replacing  $I_h^k v$  with  $\tilde{I}_h^k v$  in dealing with  $\text{I}_1$  and noting  $[\mathbf{div} \boldsymbol{\sigma}_h \cdot \mathbf{n}_F + \partial_t(\boldsymbol{\sigma}_h)_{nt}]$  is a polynomial of degree  $k-2$  on  $F \in \mathcal{F}_h(\Omega)$  in the current circumstances, we find from the second equation of (3.22) that (3.13) is recast as

$$\begin{aligned} \text{I}_1 &= \sum_{K \in \mathcal{T}_h} \int_K (f + \mathbf{div} \mathbf{div} \boldsymbol{\sigma}_h)(\psi - \tilde{I}_h^k \psi) dx - \sum_{F \in \mathcal{F}_h(\Omega)} \int_F [\mathbf{div} \boldsymbol{\sigma}_h \cdot \mathbf{n}_F \\ &\quad + \partial_t(\boldsymbol{\sigma}_h)_{nt}](\psi - \tilde{I}_h^k \psi) ds + \sum_{F \in \mathcal{F}_h(\Omega)} \int_F [(\boldsymbol{\sigma}_h)_{nn}] \{\partial_n(\psi - \tilde{I}_h^k \psi)\} ds \\ &\quad - \sum_{F \in \mathcal{F}_h} \frac{\alpha_{F,h}}{h_F} \int_F [[\boldsymbol{\nabla} u_h]] : [[\boldsymbol{\nabla}(\psi - \tilde{I}_h^k \psi)]] ds \\ &= \sum_{K \in \mathcal{T}_h} \int_K (f + \mathbf{div} \mathbf{div} \boldsymbol{\sigma}_h)(\psi - \tilde{I}_h^k \psi) dx + \sum_{F \in \mathcal{F}_h(\Omega)} \int_F [(\boldsymbol{\sigma}_h)_{nn}] \{\partial_n(\psi - \tilde{I}_h^k \psi)\} ds \\ &\quad - \sum_{F \in \mathcal{F}_h} \frac{\alpha_{F,h}}{h_F} \int_F [[\boldsymbol{\nabla} u_h]] : [[\boldsymbol{\nabla}(\psi - \tilde{I}_h^k \psi)]] ds, \end{aligned} \tag{3.25}$$

which, together with the Cauchy-Schwarz inequality and the error estimates (3.23)-(3.24) in Lemma 3.2, yields

$$|I_1| \leq C \left( \sum_{F \in \mathcal{F}_h(\Omega)} \left( \sum_{K \in \omega_F} h_K^4 \|f + \operatorname{div} \operatorname{div} \sigma_h\|_{0,K}^2 + h_F \|[(\sigma_h)_{nn}]\|_{0,F}^2 \right) + \eta_{J,h}^2(u_h) \right)^{1/2} \|\psi\|_2. \tag{3.26}$$

Combining (3.26) with (3.21) and using (3.7), we derive the following theorem:

**Theorem 3.2.** *Let  $\sigma$  and  $\sigma_h$  be solutions of the continuous problem (2.4) and the discrete problem (2.9) with  $l \geq 1$  and  $l = k - 1$  respectively. Then there exists a constant  $\tilde{C}_1$  only depending on the shape-regularity of  $\mathcal{T}_h$  and the coefficients in  $\mathcal{C}$ , such that*

$$\|\sigma - \sigma_h\|_{\mathcal{C}}^2 \leq \tilde{C}_1 \left( \tilde{\eta}_h^2(\sigma_h, f) + \eta_{h,J}^2(u_h) \right), \tag{3.27}$$

where

$$\begin{aligned} \tilde{\eta}_h^2(\sigma_h, f) &:= \tilde{\eta}_{h,1}^2(\sigma_h, f) + \eta_{h,2}^2(\sigma_h), \\ \tilde{\eta}_{h,1}^2(\sigma_h, f) &:= \sum_{F \in \mathcal{F}_h(\Omega)} \left( \sum_{K \in \omega_F} h_K^4 \|f + \operatorname{div} \operatorname{div} \sigma_h\|_{0,K}^2 + h_F \|[(\sigma_h)_{nn}]\|_{0,F}^2 \right). \end{aligned}$$

**Remark 3.1.** In fact if it is further assumed that  $k \geq 3$  on the assumption of Theorem 3.2, noting that  $\operatorname{div} \operatorname{div} \sigma_h$  is a polynomial of degree  $k - 3$  on  $K \in \mathcal{T}_h$  in this case, we may make use of the third equation of (3.22) in (3.25) and error estimates (3.23)-(3.24) to obtain

$$\begin{aligned} |I_1| &= \left| \sum_{K \in \mathcal{T}_h} \int_K (f - \bar{f}_K)(\psi - \tilde{I}_h^k \psi) dx + \sum_{F \in \mathcal{F}_h(\Omega)} \int_F [(\sigma_h)_{nn}] \{ \partial_n(\psi - \tilde{I}_h^k \psi) \} ds \right. \\ &\quad \left. - \sum_{F \in \mathcal{F}_h} \frac{\alpha_{F,h}}{h_F} \int_F [[\nabla u_h]] : [[\nabla(\psi - \tilde{I}_h^k \psi)]] ds \right| \\ &\leq C (\operatorname{osc}_h^2(f) + \sum_{F \in \mathcal{F}_h(\Omega)} h_F \|[(\sigma_h)_{nn}]\|_{0,F}^2 + \eta_{J,h}^2(u_h))^{1/2} \|\psi\|_2. \end{aligned} \tag{3.28}$$

Thus taking (3.21) into account and using (3.7) again, we arrive at

$$\|\sigma - \sigma_h\|_{\mathcal{C}}^2 \leq C_1^* (\operatorname{osc}_h^2(f) + \tilde{\eta}_h^2(\sigma_h) + \eta_{h,J}^2(u_h)) \tag{3.29}$$

with  $\tilde{\eta}_h^2(\sigma_h) := \sum_{F \in \mathcal{F}_h(\Omega)} h_F \|[(\sigma_h)_{nn}]\|_{0,F}^2 + \eta_{h,2}^2(\sigma_h)$ .

Next we prove the efficiency of the error indicator  $\eta_h^2(\sigma_h, f)$ .

**Theorem 3.3.** *Let  $\sigma$  and  $\sigma_h$  be solutions of the continuous problem (2.4) and the discrete problem (2.9) respectively. Then there exists a constant  $C_2$  only depending on the shape-regularity of  $\mathcal{T}_h$  and the coefficients in  $\mathcal{C}$ , such that*

$$C_2 \eta_h^2(\sigma_h, f) \leq \|\sigma - \sigma_h\|_{\mathcal{C}}^2 + \operatorname{osc}_h^2(f). \tag{3.30}$$

*Proof.* By virtue of (2.3) and twice elementwise integration by parts, we have a residue equation with respect to the error  $\boldsymbol{\sigma} - \boldsymbol{\sigma}_h$ : for  $v \in H_0^2(\omega_F)$

$$\begin{aligned} & \int_{\omega_F} (\boldsymbol{\sigma} - \boldsymbol{\sigma}_h) : \mathcal{K}(v) dx \\ &= \int_{\omega_F} f v dx - \sum_{K \in \omega_F} \int_K \boldsymbol{\sigma}_h : \mathcal{K}(v) dx \\ &= \sum_{K \in \omega_F} \int_K (f + \text{div div } \boldsymbol{\sigma}_h) v dx - \int_F [\text{div } \boldsymbol{\sigma}_h \cdot \mathbf{n}_F + \partial_t(\boldsymbol{\sigma}_h)_{nt}] v ds + \int_F [(\boldsymbol{\sigma}_h)_{nn}] \partial_n v ds. \end{aligned} \quad (3.31)$$

For some given element  $K \in \mathcal{T}_h$ ,  $b_K$  denotes the scaled standard third order polynomial bubble on  $K$ . Letting  $R_K = f + \text{div div } \boldsymbol{\sigma}_h$  on some  $K \in \mathcal{T}_h$  and  $\bar{R}_K = \bar{f}_K + \text{div div } \boldsymbol{\sigma}_h$ , we define  $\psi_K \in H_0^2(K)$  as  $\psi_K = \bar{R}_K b_K^2$ . The standard scaling arguments and the definition of  $\bar{R}_K$  show that

$$\begin{aligned} C \|\bar{R}_K\|_{0,K}^2 &\leq \int_K \bar{R}_K \psi_K dx \\ &= \int_K R_K \psi_K dx + \int_K (\bar{f}_K - f) \psi_K dx \\ &= \int_K (f + \text{div div } \boldsymbol{\sigma}_h) \psi_K dx + \int_K (\bar{f}_K - f) \psi_K dx. \end{aligned} \quad (3.32)$$

Invoking (3.31) with  $v = \psi_K$ , we get

$$\int_K (f + \text{div div } \boldsymbol{\sigma}_h) \psi_K dx = \int_K (\boldsymbol{\sigma} - \boldsymbol{\sigma}_h) : \mathcal{K}(\psi_K) dx. \quad (3.33)$$

Now combining (3.32) and (3.33) and using the Cauchy-Schwarz inequality, the inverse inequality, the scaling arguments and the triangle inequality give

$$Ch_K^2 \|R_K\|_{0,K} \leq \|\boldsymbol{\sigma} - \boldsymbol{\sigma}_h\|_{c,K} + h_K^2 \|f - \bar{f}_K\|_{0,K}. \quad (3.34)$$

For each edge  $F = K_1 \cap K_2 \in \mathcal{F}_h(\Omega)$ ,  $b_F$ ,  $b_{K_1}$  and  $b_{K_2}$  denote the standard bubble function with respect to  $F$ ,  $K_1$  and  $K_2$  respectively. We construct an extension of the jump  $[(\boldsymbol{\sigma}_h)_{nn}]$  to  $\omega_F$  by extending constantly along the normal to  $F$ . The resulting extension  $E([( \boldsymbol{\sigma}_h)_{nn} ])$  is a piecewise polynomial of degree  $\leq l$  on  $\omega_F$  so that  $\phi_F = (b_{K_1} - b_{K_2}) b_F^2 E([( \boldsymbol{\sigma}_h)_{nn} ]) \in H_0^2(\omega_F)$  and  $\phi_F = 0$  on  $F$ . Utilizing the scaling arguments and the residue equation (3.31) with  $v = \phi_F$ , we have

$$\begin{aligned} Ch_F^{-1} \|[(\boldsymbol{\sigma}_h)_{nn}]\|_{0,F}^2 &\leq \int_F [(\boldsymbol{\sigma}_h)_{nn}] \partial_n \phi_F ds \\ &= \sum_{K \in \omega_F} \int_K (\boldsymbol{\sigma} - \boldsymbol{\sigma}_h) : \mathcal{K}(\phi_F) dx - \sum_{K \in \omega_F} \int_K R_K \phi_F dx, \end{aligned} \quad (3.35)$$

which, together with the inverse estimate, the estimate  $\|\phi_F\|_{0,\omega_F} \leq Ch_F^{1/2} \|[(\boldsymbol{\sigma}_h)_{nn}]\|_{0,F}$  and the bound (3.34), yields

$$Ch_F^{1/2} \|[(\boldsymbol{\sigma}_h)_{nn}]\|_{0,F} \leq \sum_{K \in \omega_F} \left( \|\boldsymbol{\sigma} - \boldsymbol{\sigma}_h\|_{c,K} + h_K^2 \|f - \bar{f}_K\|_{0,K} \right). \quad (3.36)$$

For  $h_F^{3/2} \|[\mathbf{div} \boldsymbol{\sigma}_h \cdot \mathbf{n}_F + \partial_t(\boldsymbol{\sigma}_h)_{nt}]\|_{0,F}$  on some  $F = K_1 \cap K_2 \in \mathcal{F}_h(\Omega)$ , we define  $\psi_F \in H_0^2(\Omega)$  as  $256 \prod_{i=1}^2 (\lambda_{K_1 i} \lambda_{K_2 i})^2 \mathbf{E}([\mathbf{div} \boldsymbol{\sigma}_h \cdot \mathbf{n}_F + \partial_t(\boldsymbol{\sigma}_h)_{nt}])$  on  $\omega_F$  and zero on  $\Omega \setminus \omega_F$ , where  $\lambda_{K_1 i}$  and  $\lambda_{K_2 i}$ ,  $i = 1, 2$ , are barycentric coordinates of  $K_1$  and  $K_2$  associated with two end points of  $F$  respectively and  $\mathbf{E}([\mathbf{div} \boldsymbol{\sigma}_h \cdot \mathbf{n}_F + \partial_t(\boldsymbol{\sigma}_h)_{nt}])$  is given by the same process as before. We apply the arguments similar to deriving (3.35) and resort to the residue equation (3.31) with  $v = \psi_F$  to proceed

$$\begin{aligned} & C \|[\mathbf{div} \boldsymbol{\sigma}_h \cdot \mathbf{n}_F + \partial_t(\boldsymbol{\sigma}_h)_{nt}]\|_{0,F}^2 \leq ([\mathbf{div} \boldsymbol{\sigma}_h \cdot \mathbf{n}_F + \partial_t(\boldsymbol{\sigma}_h)_{nt}], \psi_F)_F \\ & = \sum_{K \in \omega_F} \left( \int_K R_K \psi_F dx - \int_K (\boldsymbol{\sigma} - \boldsymbol{\sigma}_h) : \mathcal{K}(\psi_F) dx \right) + \int_F [(\boldsymbol{\sigma}_h)_{nn}] \partial_n \psi_F ds. \end{aligned} \tag{3.37}$$

From (3.34), (3.36)-(3.37), and the inverse inequality, we know

$$\begin{aligned} & h_F^{3/2} \|[\mathbf{div} \boldsymbol{\sigma}_h \cdot \mathbf{n}_F + \partial_t(\boldsymbol{\sigma}_h)_{nt}]\|_{0,F} \\ & \leq C \left( \sum_{K \in \omega_F} (h_K^2 \|R_K\|_{0,K} + \|\boldsymbol{\sigma} - \boldsymbol{\sigma}_h\|_{C,K}) + h_F^{1/2} \|[(\boldsymbol{\sigma}_h)_{nn}]\|_{0,F} \right) \\ & \leq C \sum_{K \in \omega_F} \left( \|\boldsymbol{\sigma} - \boldsymbol{\sigma}_h\|_{C,K} + h_K^2 \|f_K - \bar{f}_K\|_{0,K} \right). \end{aligned} \tag{3.38}$$

Next we bound another two terms  $h_K \|\mathbf{rot} \mathcal{C}(\boldsymbol{\sigma}_h)\|_{0,K}$  and  $h_F^{1/2} \|[\mathcal{C}(\boldsymbol{\sigma}_h) \mathbf{t}_F]\|_{0,F}$ . As before, we are able to derive another residue equation with respect to the error  $\boldsymbol{\sigma} - \boldsymbol{\sigma}_h$ : for  $\mathbf{v} \in (H^1(\Omega))^2$

$$\begin{aligned} \int_{\Omega} \mathcal{C}(\boldsymbol{\sigma} - \boldsymbol{\sigma}_h) : \mathbf{Curl} \mathbf{v} dx &= \int_{\Omega} \mathcal{K}(u) : \mathbf{Curl} \mathbf{v} dx - \sum_{K \in \mathcal{T}_h} \int_K \mathcal{C}(\boldsymbol{\sigma}_h) : \mathbf{Curl} \mathbf{v} dx \\ &= \sum_{K \in \mathcal{T}_h} \int_K \mathbf{rot} \mathcal{C}(\boldsymbol{\sigma}_h) \cdot \mathbf{v} dx - \sum_{F \in \mathcal{F}_h} \int_F [\mathcal{C}(\boldsymbol{\sigma}_h) \mathbf{t}_F] \cdot \mathbf{v} ds. \end{aligned} \tag{3.39}$$

For some  $K \in \mathcal{T}_h$ , we define  $\boldsymbol{\phi}_K \in (H_0^1(K))^2$  as  $\boldsymbol{\phi}_K = b_K \mathbf{rot} \mathcal{C}(\boldsymbol{\sigma}_h)$ . Then, the standard scaling arguments yield

$$C \|\mathbf{rot} \mathcal{C}(\boldsymbol{\sigma}_h)\|_{0,K}^2 \leq \int_K \mathbf{rot} \mathcal{C}(\boldsymbol{\sigma}_h) \cdot \boldsymbol{\phi}_K dx. \tag{3.40}$$

So using (3.39) with  $\mathbf{v} = \boldsymbol{\phi}_K$ , (3.40), the Cauchy-Schwarz inequality, the inverse inequality, and the standard scaling arguments, we obtain

$$\begin{aligned} \|\mathbf{rot} \mathcal{C}(\boldsymbol{\sigma}_h)\|_{0,K}^2 &\leq C (\mathcal{C}(\boldsymbol{\sigma} - \boldsymbol{\sigma}_h), \mathbf{Curl} \boldsymbol{\phi}_K)_K \leq C \|\boldsymbol{\sigma} - \boldsymbol{\sigma}_h\|_{C,K} \|\mathbf{Curl} \boldsymbol{\phi}_K\|_{0,K} \\ &\leq C h_K^{-1} \|\boldsymbol{\sigma} - \boldsymbol{\sigma}_h\|_{C,K} \|\boldsymbol{\phi}_K\|_{0,K} \leq C h_K^{-1} \|\boldsymbol{\sigma} - \boldsymbol{\sigma}_h\|_{C,K} \|\mathbf{rot} \mathcal{C}(\boldsymbol{\sigma}_h)\|_{0,K}, \end{aligned}$$

i.e.,

$$C h_K \|\mathbf{rot} \mathcal{C}(\boldsymbol{\sigma}_h)\|_{0,K} \leq \|\boldsymbol{\sigma} - \boldsymbol{\sigma}_h\|_{C,K}. \tag{3.41}$$

For the last error indicator  $h_F^{1/2} \|[\mathcal{C}(\boldsymbol{\sigma}_h) \mathbf{t}_F]\|_{0,F}$  on  $F \in \mathcal{F}_h$ , we may define  $\boldsymbol{\phi}_F \in (H_0^1(\omega_F))^2$  as  $b_F h_F^{1/2} \|[\mathcal{C}(\boldsymbol{\sigma}_h) \mathbf{t}_F]\|_{0,F}$  and argue as above to get

$$C h_F^{1/2} \|[\mathcal{C}(\boldsymbol{\sigma}_h) \mathbf{t}_F]\|_{0,F} \leq \|\boldsymbol{\sigma} - \boldsymbol{\sigma}_h\|_{C,\omega_F}. \tag{3.42}$$

The desired bound results from (3.34), (3.36), (3.38), and (3.41)-(3.42). □

From Theorem 3.3, it is easy to conclude the efficiency of the estimator  $\tilde{\eta}_h^2(\sigma_h, f)$  and  $\eta_h^2(\sigma_h)$ .

**Theorem 3.4.** *Let  $\sigma$  and  $\sigma_h$  be solutions of the continuous problem (2.4) and the discrete problem (2.9) with  $l \geq 1$  and  $l = k - 1$  respectively. Then there exists a constant  $\tilde{C}_2$  only depending on the shape-regularity of  $\mathcal{T}_h$  and the coefficients in  $\mathcal{C}$ , such that*

$$\tilde{C}_2 \tilde{\eta}_h^2(\sigma_h, f) \leq \|\sigma - \sigma_h\|_{\mathcal{C}}^2 + \text{osc}_h^2(f). \tag{3.43}$$

Furthermore, when  $k \geq 3$ , there exists a constant  $C_2^*$  only depending on the shape-regularity of  $\mathcal{T}_h$  and the coefficients in  $\mathcal{C}$ , such that

$$C_2^* \tilde{\eta}_h^2(\sigma_h) \leq \|\sigma - \sigma_h\|_{\mathcal{C}}^2 + \text{osc}_h^2(f). \tag{3.44}$$

**Remark 3.2.** In the case of  $l = k - 1$  and  $k \geq 3$ , it is clear that on each  $K \in \mathcal{T}_h$

$$h_K^2 \|f - \bar{f}_K\|_{0,K} \leq h_K^2 \|f + \text{div div } \sigma_h\|_{0,K}. \tag{3.45}$$

On the other hand, with  $v = \bar{R}_K b_K \in H_0^1(K) \cap V_h^k$  on  $K$  and zero outside  $K$  in the second equation of (2.9), we do twice integration by parts to find

$$\begin{aligned} & \int_K \sigma_h : \mathcal{K}(\bar{R}_K b_K) dx + \sum_{F \subset \partial K} \int_F \{\sigma_h\} \mathbf{n}_F \cdot \nabla(\bar{R}_K b_K) ds + \sum_{F \subset \partial K} \frac{\alpha_{F,h}}{h_F} \int_F [\nabla u_h] \partial_n(\bar{R}_K b_K) ds \\ &= \int_K \text{div div } \sigma_h \cdot \nabla(\bar{R}_K b_K) dx - \int_{\partial K} \sigma_h \mathbf{n} \cdot \nabla(\bar{R}_K b_K) ds + \sum_{F \subset \partial K} \int_F \{\sigma_h\} \mathbf{n}_F \cdot \nabla(\bar{R}_K b_K) ds \\ & \quad + \sum_{F \subset \partial K} \frac{\alpha_{F,h}}{h_F} \int_F [\nabla u_h] \partial_n(\bar{R}_K b_K) ds \\ &= - \int_K \text{div div } \sigma_h \bar{R}_K b_K dx - \frac{1}{2} \sum_{F \subset \partial K} \int_F [\sigma_h] \cdot \nabla(\bar{R}_K b_K) ds + \sum_{F \subset \partial K} \frac{\alpha_{F,h}}{h_F} \int_F [\nabla u_h] \partial_n(\bar{R}_K b_K) ds \\ &= \int_K f \bar{R}_K b_K dx, \end{aligned}$$

i.e.,

$$\begin{aligned} & - \frac{1}{2} \sum_{F \subset \partial K} \int_F [(\sigma_h)_{nn}] \partial_n(\bar{R}_K b_K) ds + \sum_{F \subset \partial K} \frac{\alpha_{F,h}}{h_F} \int_F [\nabla u_h] \partial_n(\bar{R}_K b_K) ds \\ &= \int_K (f + \text{div div } \sigma_h) \bar{R}_K b_K dx. \end{aligned} \tag{3.46}$$

As arguing in (3.32), we deduce with the help of (3.46)

$$\begin{aligned} C \|\bar{R}_K\|_{0,K}^2 &\leq \int_K \bar{R}_K^2 b_K dx = \int_K R_K \bar{R}_K b_K dx + \int_K (\bar{f}_K - f) \bar{R}_K b_K dx \\ &= \int_K (f + \text{div div } \sigma_h) \bar{R}_K b_K dx + \int_K (\bar{f}_K - f) \bar{R}_K b_K dx \\ &= - \frac{1}{2} \sum_{F \subset \partial K} \int_F [(\sigma_h)_{nn}] \partial_n(\bar{R}_K b_K) ds + \sum_{F \subset \partial K} \frac{\alpha_{F,h}}{h_F} \int_F [\nabla u_h] \partial_n(\bar{R}_K b_K) ds \\ & \quad + \int_K (\bar{f}_K - f) \bar{R}_K b_K dx, \end{aligned} \tag{3.47}$$

which, along with the Cauchy-Schwarz inequality, the scaling arguments, and the triangle inequality, implies

$$\begin{aligned}
 & h_K^2 \|f + \operatorname{div} \operatorname{div} \boldsymbol{\sigma}_h\|_{0,K} \\
 & \leq C \left( h_K^2 \|f - \bar{f}_K\|_{0,K} + \sum_{F \subset \partial K} (h_F^{1/2} \|[(\boldsymbol{\sigma}_h)_{nn}]\|_{0,F} + \frac{\alpha_{F,h}}{h_F^{1/2}} \|[\nabla u_h]\|_{0,F}) \right). \tag{3.48}
 \end{aligned}$$

Now from (3.45) and (3.48), we find two quantities

$$\tilde{\eta}_{h,1}^2(\boldsymbol{\sigma}_h, f) + \eta_{h,J}^2(u_h), \quad \operatorname{osc}_h^2(f) + \sum_{F \in \mathcal{F}_h(\Omega)} h_F \|[(\boldsymbol{\sigma}_h)_{nn}]\|_{0,F}^2 + \eta_{h,J}^2(u_h)$$

are equivalent.

### 4. Numerical Experiments

In this section we report two numerical examples to validate the effectiveness of the proposed error estimator. First an adaptive local  $C^0$  discontinuous Galerkin (ALCDG) method for the Kirchhoff bending plate is presented on the basis of the mixed formulation (2.9) and the error estimator. In the following algorithm, all dependence on triangulation  $\mathcal{T}_h$  is now replaced by the iteration counter  $m$ . Define

$$\begin{aligned}
 \bar{\eta}_m^2(\boldsymbol{\sigma}_m, u_m, f, F) & := \eta_m^2(\boldsymbol{\sigma}_m, f, F) + \eta_{m,J}^2(u_m, F) \quad \forall F \in \mathcal{F}_m, \\
 \bar{\eta}_m^2(\boldsymbol{\sigma}_m, u_m, f, \mathcal{S}_m) & := \sum_{F \in \mathcal{S}_m} \bar{\eta}_m^2(\boldsymbol{\sigma}_m, u_m, f, F) \quad \forall \mathcal{S}_m \subseteq \mathcal{F}_m, \\
 \bar{\eta}_m^2(\boldsymbol{\sigma}_m, u_m, f) & := \bar{\eta}_m^2(\boldsymbol{\sigma}_m, u_m, f, \mathcal{F}_m).
 \end{aligned}$$

**Algorithm 4.1.** *ALCDG*

Given a parameter  $0 < \theta < 1$  and an initial mesh  $\mathcal{T}_0$ . Set  $m := 0$ .

1. (SOLVE) Solve the discrete problem (2.9) on  $\mathcal{T}_m$  for the discrete solution  $(\boldsymbol{\sigma}_m, u_m) \in \boldsymbol{\Sigma}_m^l \times V_m^k$ .
2. (ESTIMATE) Compute the error indicator  $\{\bar{\eta}_m^2(\boldsymbol{\sigma}_m, u_m, f, F)\}_{F \in \mathcal{F}_m}$ .
3. (MARK) Mark a set  $\mathcal{S}_m \subset \mathcal{F}_m$  with minimal cardinality such that

$$\bar{\eta}_m^2(\boldsymbol{\sigma}_m, u_m, f, \mathcal{S}_m) \geq \theta \bar{\eta}_m^2(\boldsymbol{\sigma}_m, u_m, f).$$

4. (REFINE) Refine each triangle  $K$  with at least one edge in  $\mathcal{S}_m$  by the newest vertex bisection to get  $\mathcal{T}_{m+1}$ .
5. Set  $m := m + 1$  and go to Step 1.

Now we test the above algorithm on three examples, in all of which, we choose  $\theta = 0.6, \nu = 0.3$  and take  $E, d$  such that

$$Ed^3 = 12(1 - \nu^2).$$

With this choice, it follows

$$\mathcal{M}(u) = (1 - \nu)\mathcal{K}(u) + \nu \operatorname{tr}(\mathcal{K}(u))\mathcal{I},$$

$$\mathcal{C}(\boldsymbol{\sigma}) = \frac{1}{1-\nu}\boldsymbol{\sigma} - \frac{\nu}{1-\nu^2}\text{tr}(\boldsymbol{\sigma})\mathcal{I}.$$

**Example 4.1.** In this example, let  $\Omega = (-1, 1) \times (-1, 1)$  and

$$u(x, y) = (x^2 - 1)^2(y^2 - 1)^2e^{-5(x^2+y^2)}.$$

$f(x, y)$  is computed by the first equation of (2.1). Polynomial degrees are chosen as  $l = 0$  and  $k = 2$ . Fig. 4.1 shows meshes generated successively by Algorithm 4.1. The top-left one of Fig. 4.1 is the initial mesh  $\mathcal{T}_0$ . The top-right, bottom-left and bottom-right ones of Fig. 4.1 represent meshes generated by the adaptive algorithm for  $m = 6, 9, 12$  respectively. From Fig. 4.1, we find that singularities of the solution are detected by the adaptive process. Detailed numerical results are given in Table 4.1, in which #DOFs stands for the number of degrees of freedom. It is discovered from the last column of Table 4.1 that as the algorithm proceeds the computed effectivity index remains a constant, which quantifies the overestimation of the error estimator. The true error and the error estimator are depicted in Fig. 4.2 as functions of the number of DOFs on the mesh sequence generated by the adaptive algorithm in a ln-ln scale. We observe an optimal convergence rate  $\|\boldsymbol{\sigma} - \boldsymbol{\sigma}_m\|_c = O((\#\text{DOFs})^{-1/2})$ .

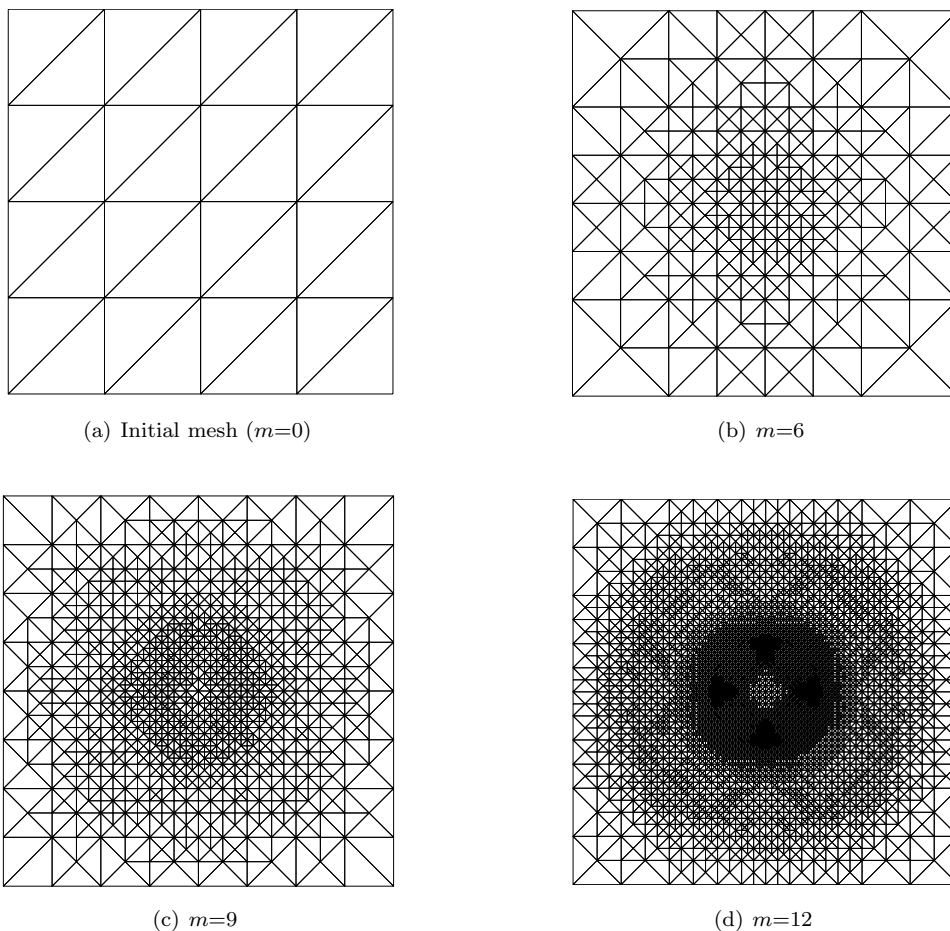


Fig. 4.1. Meshes generated in ALCDG with different  $m$  for Example 4.1.

Table 4.1: Number of DOFs, energy-norm error, error estimator, and effectivity index in Example 4.1.

$m$	#DOFs	$\ \sigma - \sigma_m\ _C$	$\bar{\eta}_m(\sigma_m, u_m, f)$	$\bar{\eta}_m / \ \sigma - \sigma_m\ _C$
0	49	7.9760E+00	5.9648E+01	7.48
1	89	6.4339E+00	3.2296E+01	5.02
2	141	4.0420E+00	1.8274E+01	4.52
3	217	2.8074E+00	1.1347E+01	4.04
4	325	2.2937E+00	8.2861E+00	3.61
5	541	1.8029E+00	5.8119E+00	3.22
6	861	1.4648E+00	4.4208E+00	3.02
7	1481	1.0984E+00	3.2148E+00	2.93
8	2453	8.5371E-01	2.4373E+00	2.86
9	3989	6.6239E-01	1.8673E+00	2.82
10	6477	5.3485E-01	1.4669E+00	2.74
11	11045	4.0873E-01	1.1175E+00	2.73
12	18985	3.0789E-01	8.4458E-01	2.74
13	31221	2.3721E-01	6.4669E-01	2.73

**Example 4.2.** In this example we consider a problem with a corner singularity in the solution [26].  $\Omega$  is taken to be an L-shaped domain  $\Omega = (-1, 1) \times (-1, 1) \setminus [0, 1) \times (-1, 0]$  and the exact singular solution

$$u(r, \theta) = (r^2 \cos^2 \theta - 1)^2 (r^2 \sin^2 \theta - 1)^2 r^{(1+z)} g(\theta),$$

where  $z = 0.544483736782464$  is a noncharacteristic root of  $\sin^2(z\omega) = z^2 \sin^2 \omega, \omega = \frac{3\pi}{2}$  and

$$g(\theta) = \left( \frac{1}{z-1} \sin((z-1)\omega) - \frac{1}{z+1} \sin((z+1)\omega) \right) \times (\cos((z-1)\theta) - \cos((z+1)\theta)) - \left( \frac{1}{z-1} \sin((z-1)\theta) - \frac{1}{z+1} \sin((z+1)\theta) \right) \times (\cos((z-1)\omega) - \cos((z+1)\omega)).$$

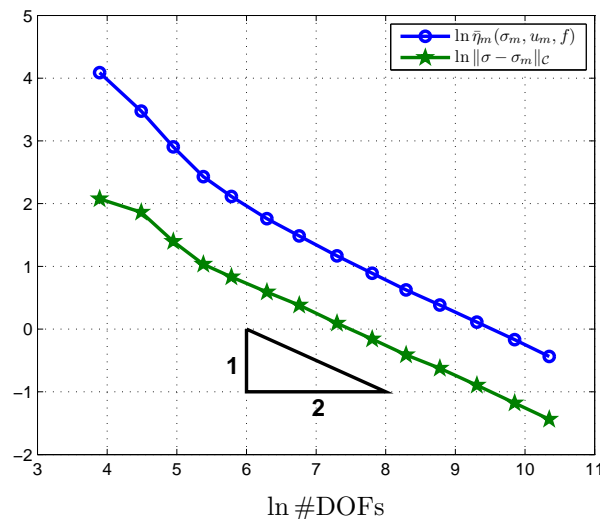


Fig. 4.2. Estimator, energy error vs #DOFs in ln–ln scale for Example 4.1.

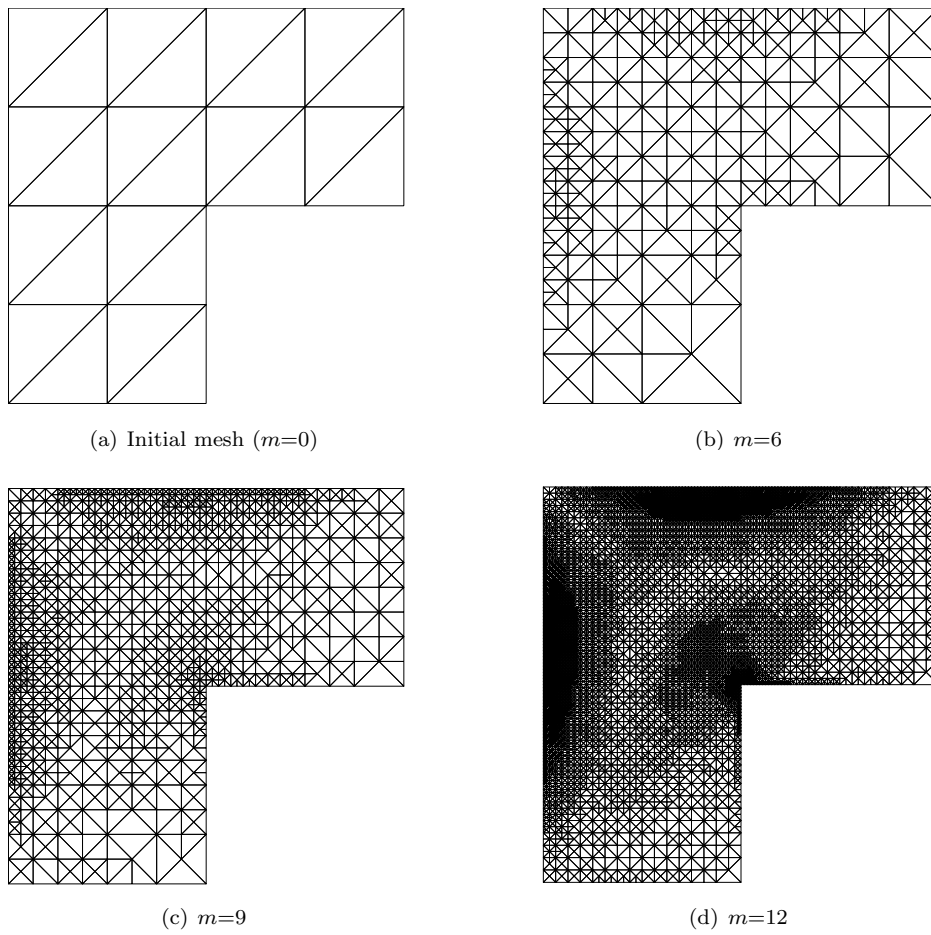


Fig. 4.3. Meshes generated in ALCDG with different  $m$  for Example 4.2.

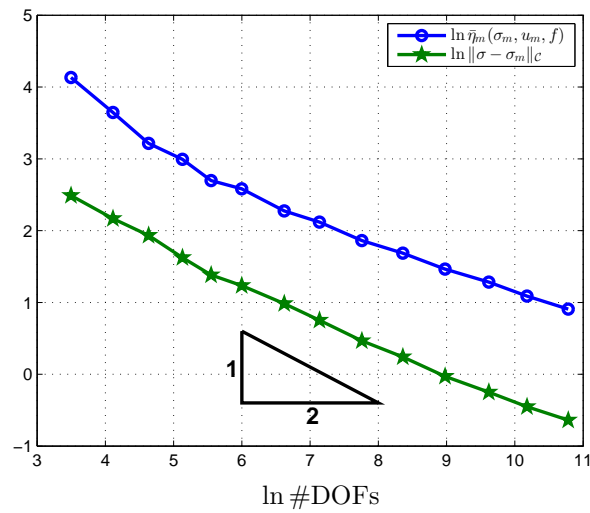


Fig. 4.4. Estimator, energy error vs #DOFs in ln–ln scale for Example 4.2.

Table 4.2: Number of DOFs, energy-norm error, error estimator, and effectivity index in Example 4.2.

$m$	#DOFs	$\ \sigma - \sigma_m\ _C$	$\bar{\eta}_m(\sigma_m, u_m, f)$	$\bar{\eta}_m / \ \sigma - \sigma_m\ _C$
0	33	1.2053E+01	6.2302E+01	5.17
1	61	8.7286E+00	3.8272E+01	4.38
2	103	6.9163E+00	2.4909E+01	3.60
3	169	5.0710E+00	1.9940E+01	3.93
4	257	3.9881E+00	1.4836E+01	3.72
5	403	3.4390E+00	1.3240E+01	3.85
6	751	2.6713E+00	9.7210E+00	3.64
7	1259	2.1220E+00	8.3243E+00	3.92
8	2341	1.5939E+00	6.4288E+00	4.03
9	4266	1.2731E+00	5.4015E+00	4.24
10	7914	9.7111E-01	4.3264E+00	4.46
11	15039	7.7946E-01	3.6073E+00	4.63
12	26311	6.3685E-01	2.9681E+00	4.66
13	48117	5.2806E-01	2.4767E+00	4.69

Polynomial degrees  $l$  and  $k$  are also set equal to 0 and 2 respectively. The initial mesh  $\mathcal{T}_0$  is drawn in the top-left one of Fig. 4.3. The top-right, bottom-left and bottom-right ones of Fig. 4.3 show meshes generated by the adaptive algorithm for  $m = 6, 9, 12$  respectively. We observe that singularities around the re-entrant corner are captured accurately. Numerical results are given in Table 4.2. As previously, the computed effectivity index tends to a constant as the algorithm proceeds. Finally, the history of the error and the estimator versus the number of DOFs in a ln-ln scale is shown in Fig. 4.4, which indicates that  $\|\sigma - \sigma_m\|_C = O((\#\text{DOFs})^{-s})$  for some  $s \in (0.3, 0.5)$ .

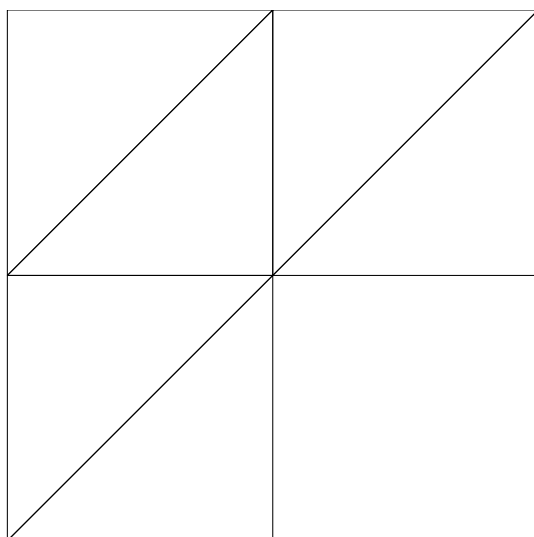


Fig. 4.5. Initial mesh for Example 4.3.

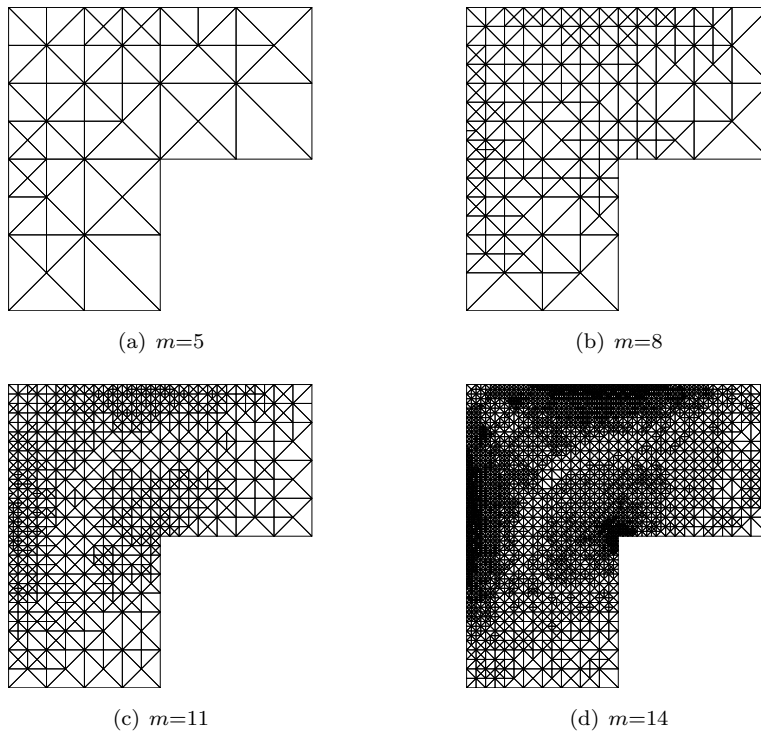


Fig. 4.6. Meshes generated in ALCDG with  $\bar{\eta}_m(\sigma_m, u_m, f)$  and different  $m$  for Example 4.3.

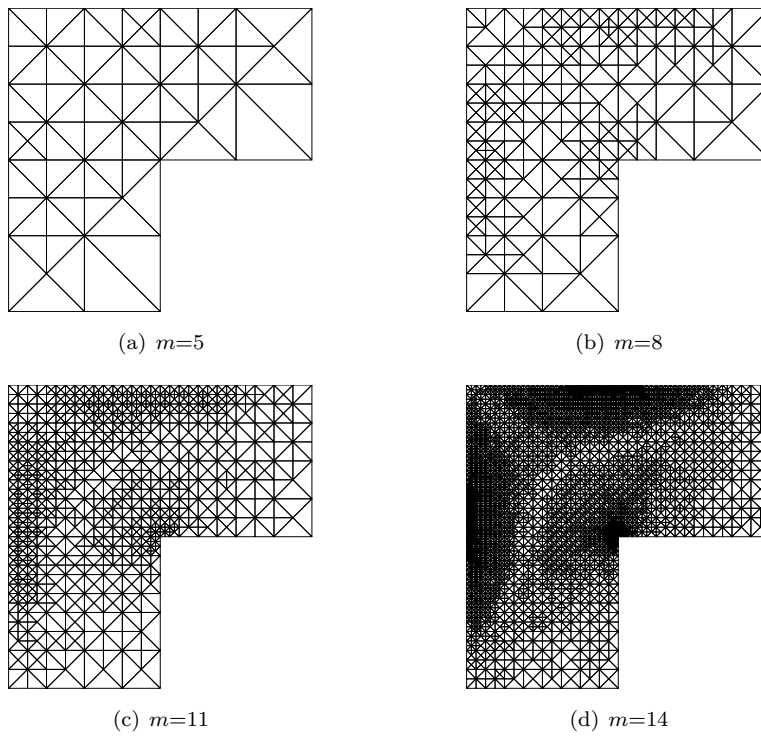


Fig. 4.7. Meshes generated in ALCDG with  $\tilde{\eta}_m^2(\sigma_m, u_m, f)$  and different  $m$  for Example 4.3.

Table 4.3: Comparison of number of DOFs, error estimator and effectivity index in Example 4.3.

$m$	#DOFs	$\bar{\eta}_m(\boldsymbol{\sigma}_m, u_m, f)$	$\bar{\eta}_m/\ \boldsymbol{\sigma} - \boldsymbol{\sigma}_m\ _0$	#DOFs	$\tilde{\eta}_m(\boldsymbol{\sigma}_m, u_m, f)$	$\tilde{\eta}_m/\ \boldsymbol{\sigma} - \boldsymbol{\sigma}_m\ _0$
1	13	1.6750E+02	16.9	13	1.3844E+02	15.7
2	28	9.3837E+01	12.0	28	6.5805E+01	11.0
3	45	6.4397E+01	8.09	41	4.5304E+01	7.46
4	71	4.4010E+01	6.69	71	2.9468E+01	5.81
5	127	3.2291E+01	5.01	135	1.9358E+01	4.42
6	199	2.3017E+01	4.21	217	1.5126E+01	3.40
7	341	1.9255E+01	4.10	353	1.2050E+01	3.36
8	580	1.4625E+01	3.88	585	9.7598E+00	3.13
9	942	1.1325E+01	3.66	991	7.6159E+00	3.02
10	1598	9.3919E+00	3.69	1641	6.0735E+00	3.04
11	2687	7.3761E+00	3.56	2875	4.7596E+00	2.87
12	4674	5.9432E+00	3.51	4802	3.7905E+00	2.85
13	8350	4.4915E+00	3.43	8570	2.8890E+00	2.78
14	14014	3.5669E+00	3.28	15073	2.2658E+00	2.63

**Example 4.3.** The final example is to compare computing performance of  $\bar{\eta}_m(\boldsymbol{\sigma}_m, u_m, f)$  and  $\tilde{\eta}_m(\boldsymbol{\sigma}_m, u_m, f) = (\tilde{\eta}_m^2(\boldsymbol{\sigma}_m, f) + \eta_{m,J}^2(u_m))^{1/2}$ . We implement Algorithm 4.1 using these two estimators respectively on the same problem as in Example 4.2. Let  $l = 1$ ,  $k = 2$  and set the initial mesh as in Fig. 4.5.

Fig. 4.6 and Fig. 4.7 display meshes generated by the adaptive algorithm for  $m = 5, 8, 11, 14$  respectively. As in Example 4.2, the singularities of the solution are detected in the vicinity of the re-entrant corner and near the edges in the refinement process. Numerical results for two a posteriori error estimators are reported in Table 4.3. We find that two estimators  $\bar{\eta}_m(\boldsymbol{\sigma}_m, u_m, f)$  and  $\tilde{\eta}_m(\boldsymbol{\sigma}_m, u_m, f)$  both overestimate the error but the computed effectivity index for the latter is about 20% less than that for the former. It is clear that ALCDG with the improved estimator in Theorem 3.2 provides better approximations of the true solution.

**Acknowledgements.** The authors thank the referees for their valuable comments leading to great improvement of the earlier version of the paper. This work was partially supported by the National Natural Science Foundation of China (11171219, 11201307, 11301396), China MOE Specialized Research Fund for the Doctoral Program of Higher Education (20123127120001), E-Institutes of Shanghai Municipal Education Commission (E03004), and Innovation Program of Shanghai Municipal Education Commission (13YZ059).

## References

- [1] M. Ainsworth, A posteriori error estimation for discontinuous Galerkin finite element approximation, *SIAM J. Numer. Anal.*, **45** (2007), 1777-1798.
- [2] D. N. Arnold, F. Brezzi, B. Cockburn, and L. D. Marini, Unified analysis of discontinuous Galerkin methods for elliptic problems, *SIAM J. Numer. Anal.*, **39** (2002), 1749-1779.
- [3] I. Babuška and M. Zlámal, Nonconforming elements in the finite element method with penalty, *SIAM J. Numer. Anal.*, **10** (1973), 863-875.
- [4] G. A. Baker, Finite element methods for elliptic equations using nonconforming elements, *Math. Comp.*, **31** (1977), 45-59.

- [5] R. Becker, P. Hansbo, and M. G. Larson, Energy norm a posteriori error estimation for discontinuous Galerkin methods, *Comput. Methods Appl. Mech. Engrg.*, **192** (2003), 723-733.
- [6] L. Beirão da Veiga, J. Niiranen, and R. Stenberg, A posteriori error estimates for the Morley plate bending element, *Numer. Math.*, **106** (2007), 165-179.
- [7] L. Beirão da Veiga, J. Niiranen, and R. Stenberg, A posteriori error analysis for the Morley plate element with general boundary conditions, *Int. J. Numer. Methods Eng.*, **83** (2010), 1-26.
- [8] S. C. Brenner, T. Gudi, and L. Sung, An a posteriori error estimator for a quadratic  $C^0$ -interior penalty method for the biharmonic problem, *IMA J. Numer. Anal.*, **30** (2010), 777-798.
- [9] S. C. Brenner and L. R. Scott, *The Mathematical Theory of Finite Element Methods* (Third Edition), Springer, New York, 2008.
- [10] S. C. Brenner and L. Sung,  $C^0$  interior penalty methods for fourth order elliptic boundary value problems on polygonal domains, *J. Sci. Comp.*, **22/23** (2005), 83-118.
- [11] F. Brezzi, B. Cockburn, L. D. Marini, and E. Süli, Stabilization mechanisms in discontinuous Galerkin finite element methods, *Comput. Methods Appl. Mech. Engrg.*, **195** (2006), 3293-3310.
- [12] F. Brezzi and M. Fortin, *Mixed and Hybrid Finite Element Methods*, Springer-Verlag, New York, 1991.
- [13] R. Bustinza, G. Gatica, and B. Cockburn, An a posteriori error estimate for the local discontinuous Galerkin method applied to linear and nonlinear diffusion problems, *J. Sci. Comp.*, **22/23** (2005), 147-185.
- [14] C. Carstensen, T. Gudi, and M. Jensen, A unifying theory of a posteriori error control for discontinuous Galerkin FEM, *Numer. Math.*, **112** (2009), 363-379.
- [15] P. Castillo, An a posteriori error estimate for the local discontinuous Galerkin method, *J. Sci. Comp.*, **22/23** (2005), 187-204.
- [16] P. Castillo, B. Cockburn, I. Perugia, and D. Schötzau, An a priori error analysis of the local discontinuous Galerkin method for elliptic problems, *SIAM J. Numer. Anal.*, **18** (2000), 1676-1706.
- [17] P. G. Ciarlet, *The Finite Element Method for Elliptic Problems*, North-Holland, Amsterdam, 1978.
- [18] B. Cockburn, Discontinuous Galerkin methods, *ZAMM Z. Angew. Math. Mech.*, **83** (2003), 731-754.
- [19] B. Cockburn, B. Dong, and J. Guzmán, A hybridizable and superconvergent discontinuous Galerkin method for biharmonic problems, *J. Sci. Comput.*, **40** (2009), 141-187.
- [20] B. Cockburn and C.-W. Shu, The local discontinuous Galerkin method for time-dependent convection-diffusion systems, *SIAM J. Numer. Anal.*, **35** (1998), 2440-2463.
- [21] B. Cockburn, G. E. Karniadakis, and C.-W. Shu (eds.), *Discontinuous Galerkin methods. Theory, computation and applications*, *Lecture Notes in Computational Science and Engineering*, vol. 11, Springer, Berlin-Heidelberg-New York, 2000.
- [22] J. Jr. Douglas, T. Dupont, P. Percell, and R. Scott, A family of  $C^1$  finite element with optimal approximation properties for various Galerkin methods for 2nd and 4th order problems, *R.A.I.R.O., Anal. Numér.*, **13** (1979), 227-255.
- [23] G. Engel, K. Garikipati, T. J. R. Hughes, M. G. Larson, L. Mazzei, and R. L. Taylor, Continuous/discontinuous finite element approximations of fourth-order elliptic problems in structural and continuum mechanics with applications to thin beams and plates, and strain gradient elasticity, *Comput. Methods Appl. Mech. Engrg.*, **191** (2002), 3669-3750.
- [24] E. H. Georgoulis and P. Houston, Discontinuous Galerkin methods for the biharmonic problem, *IMA J. Numer. Anal.*, **29** (2009), 573-594.
- [25] E. H. Georgoulis, P. Houston, and J. Virtanen, An a posteriori error indicator for discontinuous Galerkin approximations of fourth order elliptic problems, *IMA J. Numer. Anal.*, **31** (2011), 281-298.
- [26] P. Grisvard, *Singularities in Boundary Value Problems*, Masson, Paris, 1992.

- [27] P. Hansbo and M. G. Larson, A discontinuous Galerkin method for the plate equation, *Calcolo*, **39** (2002), 41-59.
- [28] P. Hansbo and M. G. Larson, A posteriori error estimates for continuous/discontinuous Galerkin approximations of the Kirchhoff-Love plate, *Comput. Methods Appl. Mech. Engrg.*, **200** (2011), 3289-3295.
- [29] P. Houston, D. Schötzau, and T. P. Wihler, Energy norm a posteriori error estimation of  $hp$ -adaptive discontinuous Galerkin methods for ellipt problems, *Math. Models Methods Appl. Sci.*, **17** (2007), 33-62.
- [30] J. Hu and Z. Shi, A new a posteriori error estimate for the Morley element, *Numer. Math.*, **112** (2009), 25-40.
- [31] J. Huang, X. Huang, and W. Han, A new  $C^0$  discontinuous Galerkin method for Kirchhoff plates, *Comput. Methods Appl. Meth. Engrg.*, **199** (2010), 1446-1454.
- [32] O. A. Karakashian and F. Pascal, A posteriori error estimates for a discontinuous Galerkin approximation of second-order elliptic problems, *SIAM J. Numer. Anal.*, **41** (2003), 2374-2399.
- [33] L. S. D. Morley, The triangular equilibrium element in the solution of plate bending problems, *Aero. Quart.*, **19** (1968), 149-169.
- [34] I. Mozolevski and P. R. Bösing, Sharp expressions for the stabilization parameters in symmetric interior-penalty discontinuous Galerkin finite element approximations of fourth-order elliptic problems, *Comput. Methods Appl. Math.*, **7** (2007), 365-375.
- [35] I. Mozolevski and E. Süli, A priori error analysis for the  $hp$ -version of the discontinuous Galerkin finite element method for the biharmonic equation, *Comput. Methods Appl. Math.*, **3** (2003), 596-607.
- [36] I. Mozolevski, E. Süli, and P. R. Bösing,  $hp$ -version a priori error analysis of interior penalty discontinuous Galerkin finite element approximations to the biharmonic equation, *J. Sci. Comput.*, **30** (2007), 465-491.
- [37] B. Rivière and M. Wheeler, A posteriori error estimates for a discontinuous Galerkin method applied to elliptic problems, *Comput. Math. Appl.*, **46** (2003), 141-163.
- [38] L. R. Scott and S. Zhang, Finite element interpolation of nonsmooth functions satisfying boundary conditions, *Math. Comp.*, **54** (1990), 483-493.
- [39] E. Süli and I. Mozolevski,  $hp$ -version interior penalty DGFEMs for the biharmonic equation, *Comput. Methods Appl. Mech. Engrg.*, **196** (2007), 1851-1863.
- [40] R. Verfürth, A Review of A Posteriori Estimation and Adaptive Mesh-Refinement Techniques, Wiley-Teubner, Chichester, New York, Stuttgart, 1996.
- [41] G. N. Wells and N. T. Dung, A  $C^0$  discontinuous Galerkin formulation for Kirchhoff plates, *Comput. Methods Appl. Mech. Engrg.*, **196** (2007), 3370-3380.